Published in final edited form as:
Kidney Int. 2008 December ; 74(12): 1548–1556. doi:10.1038/ki.2008.411.

Parathyroid-specific interaction of the calcium-sensing receptor and Gaq

Min Pi[1], **Ling Chen**[1], **MinZhao Huang**[1], **Qiang Luo**[1], and **L. Darryl Quarles**[1]
[1]The Kidney Institute, University of Kansas Medical Center, Kansas City, Kansas, USA

Abstract

The calcium-sensing receptor regulates various parathyroid gland functions, including hormone secretion, gene transcription, and chief cell hyperplasia through Gαq- and Gαi-dependent signaling pathways. To determine the specific function of Gαq in these processes, we generated transgenic mice using the human parathyroid hormone promoter to drive overexpression of a dominant negative Gαqloop minigene to selectively disrupt Gαq function in the parathyroid gland. The Gαqloop mRNA was highly expressed in the parathyroid gland but not in other tissues of these transgenic mice. Gross appearance, body weight, bone mineral density, and survival of the transgenic mice were indistinguishable from those of their wild-type littermates. Adult transgenic mice, however, exhibited an increase in parathyroid hormone mRNA and in its basal serum level as well as in gland size. The response of the parathyroid gland to hypocalcemia was found to be reduced in sensitivity in the transgenic mice when compared to their wild-type controls. Abnormalities of the parathyroid gland function in these transgenic mice were similar to those of heterozygous $G\alpha q^{+/-}$ and calcium sensing $receptor^{+/-}$ mice. These studies demonstrate the feasibility of selectively targeting the parathyroid gland to investigate signaling mechanisms downstream of the calcium receptor.

Keywords

calcium-sensing receptor; G-protein; parathyroid gland

The parathyroid gland synthesizes and secretes parathyroid hormone (PTH) in response to changes in serum-ionized calcium concentrations. Extracellular calcium is sensed by calcium-sensing receptor (CASR), a 7-transmembrane domain G-protein-coupled receptor, which is located predominately in parathyroid chief cells.[1-3] CASR regulates serum PTH levels by controlling many aspects of parathyroid gland function, including PTH secretion, PTH gene transcription, and parathyroid cell growth. CASR senses small changes in extracellular calcium and regulates serum PTH levels to maintain the serum calcium levels in a narrow range. Ablation of CASR in mice results in hyperparathyroidism[4] and the respective heterozygous and homozygous inactivating mutation of CASR in humans causes familial hypocalciuric hypercalcemia and neonatal severe hyperparathyroidism.[4-6] In contrast, hypoparathyroidism, which is characterized by low circulating PTH levels, results from activating mutations of CASR.[7] These mouse genetic models and human hereditary disorders establish CASR as essential for regulating parathyroid gland function and maintaining calcium home-ostasis.

Correspondence: Min Pi, The Kidney Institute, University of Kansas Medical Center, 3901 Rainbow Boulevard, 6020H Wahl Hall East, Kansas City, Kansas 66160, USA. E-mail: mpi@kumc.edu L. Darryl Quarles, The Kidney Institute, University of Kansas Medical Center, 3901 Rainbow Boulevard, 6020H Wahl Hall East, Kansas City, Kansas 66160, USA. E-mail: dquarles@kumc.edu.

DISCLOSURE
The authors stated no conflict of interest.

Acquired hypocalcemic disorders, such as chronic kidney disease and vitamin D deficiency, cause secondary hyperparathyroidism, which is characterized by elevated circulating PTH levels, increased PTH production per cell (hypertrophy), and parathyroid gland hyperplasia. Activation of CASR with calcimimetics has proven to be a successful treatment of secondary hyperparathyroidism in Chronic kidney disease.[8,9]

Additional advances in treating hyperparathyroidism may be derived from a greater knowledge of the cellular functions of the specific signaling pathways coupled to CASR in the parathyroid gland. Studies in heterologous cell culture systems have shown that CASR is coupled to Gαi,[10] Gαq,[11] and Gα12/13.[12] CASR-mediated activation of Gαi and Gαq results in the inhibition of agonist-induced cAMP accumulation and stimulation of PI-PLC-mediated increments in inositol trisphosphate, diacylglycerol, and intracellular calcium.[13,14] CASR also activates phospholipase A2,[14,15] phospholipase D, extracellular signal-regulated kinase,[4,13-17] and Rho-dependent pathways[18-20] in nonparathyroid cells systems. CASR signaling is inhibited by GRK4-dependent receptor phosphorylation and *β*-arrest-in2-dependent desensitization in HEK-293 cells.[19] As primary parathyroid cell cultures do not retain their phenotype when grown under conditions required to selectively manipulate specific signaling pathways and are difficult to transfect, it has not been possible to elucidate the separate functions of Gαq and Gαi-dependent signaling by directly manipulating their expression in the parathyroid cells *ex vivo*. This is an important limitation, as Gα subunits are known to regulate both distinct and overlapping effector pathways and biological functions in a cell-type-specific fashion.[21] For example, Gαq in many cell systems stimulates proliferation/hyperplasia by activation of Raf/ERK1/2 pathways. In other cell types, Gαq family members promote apoptosis by intracellular calcium/calcineurin-dependent and/or RhoA-dependent pathways.[22] In contrast, activation of Gαi, which reduces cAMP production, exerts anti-proliferative actions in most cell systems, but can paradoxically stimulate proliferation in cells that express the PKA responsive B-Raf isoform.[23,24]

In the current studies, we evaluated the function of Gαq in the parathyroid gland by creating a transgenic mouse line ($Tg^{PTHp–Gqloop}$) in which the PTH promoter drives the expression of the C-terminal peptide of Gαq, which acts as a dominant negative, specific inhibitor specific for Gαq.

RESULTS

CASR is coupled to Gαq and Gαi, and the dominant-negative Gαqloop minigene blocks CASR-mediated signaling pathway *in vitro*

Initially, we examined the role of Gαq and Gαi in mediating the actions of CASR in HEK-293 cells that coexpress CASR and an SRE-promoter-luciferase reporter construct. CASR-and SRE-luc-expressing HEK-293 cells were transfected with a cDNA encoding the dominant-negative Gαqloop minigene. This minigene that encodes a C-terminal peptide sequence of mouse Gαq, residues 305−359, has previously been shown to selectively disrupt Gαq *in vitro* and *in vivo*.[25] We found that extracellular calcium significantly stimulated SRE-luc activity in the absence of the Gαqloop minigene. In contrast, calcium-stimulated SRE-luc was significantly inhibited by the overexpression of the Gαqloop in CASR-expressing HEK-293 cells (Figure 1). In addition, pretreatment with pertussis toxin, a selective irreversible inactivator of Gαi/Gαo,[26] also significantly inhibited extracellular calcium stimulation of SRE-luciferase CASR-expressing HEK-293 cells (Figure 1). Combined Gαqloop overexpression and treatment with pertussis toxin had additive effects on CASR-stimulated SRE activity (Figure 1), consistent with CASR coupling to both Gαq- and Gαi-dependent pathways.

Creation of $Tg^{PTHp–Gqloop}$ transgenic mice

Next, we overexpressed the dominant-negative Gαqloop minigene[25] in mice using a PTH promoter construct to achieve class-specific inhibition of Gαq in selectively in the parathyroid gland *in vivo*. The targeting strategy that we used is shown in Figure 2a. Wild-type and $Tg^{PTHp–Gqloop}$ transgenic mice were genotyped by PCR (Figure 2b) and found to be born at the expected Mendelian frequency. In addition, the survival, gross appearance, body weight, and bone mineral density of $Tg^{PTHp–Gqloop}$ transgenic mice were indistinguishable from wild-type mice (data not shown). The expression of the Gαqloop transgene was highly and selectively expressed in the parathyroid/thyroid tissue (Figure 2c and d). We failed to detect the transgene in any other tissue, including the heart, lung, liver, kidney, and thymus (Figure 2c). In addition, using a C-terminal antibody to Gαq, we confirmed the expression of the Gαqloop peptide in protein isolated from the parathyroid/thyroid tissues (Figure 2d). The high ratio of the intact Gαq to the Gαqloop peptide likely reflects the disproportionate contribution of the thyroid gland, which expresses Gαq but not the Gαqloop transgene (Figure 2c). We failed to detect the peptide in tissues outside the parathyroid gland (data not shown).

Elevated basal PTH levels in $Tg^{PTHp–Gqloop}$ transgenic mice

We initially examined the effect of the dominant-negative overexpression of the Gαqloop minigene on basal serum PTH, calcium and phosphorus levels (Table 1). We found a significant, ~2-fold increase in serum PTH levels in $Tg^{PTHp–Gqloop}$ transgenic mice compared to wild-type controls (Table 1). However, we did not detect differences in either serum calcium or phosphate in $Tg^{PTHp–Gqloop}$ transgenic mice. In addition, we also did not detect any difference in urinary calcium/creatinine ratio or urinary phosphorus/creatinine ratio between wild-type and transgenic mice (data not shown).

To gain insights into the degree of Gαqloop-dependent disruption of Gαq in the PTG and the possible differences between parathyroid-specific targeting of Gαq and global Gαq-deficient mice, we compared $Tg^{PTHp–Gqloop}$ transgenic mice with Gαq-deficient mice.[27] These comparisons were limited to heterozygous Gαq mutant mice $Gαq^{+/–}$,[27] as homozygous $Gαq^{–/–}$ mice are embryonic lethal. We observed a similar twofold increase in basal serum PTH levels in 8-week-old $Gαq^{+/–}$ mice compared to wild-type littermates, without changes in serum calcium or phosphorus (Table 1), urinary calcium/creatinine ratio or phosphorus/creatinine (data not shown).

We also compared $Tg^{PTHp–Gqloop}$ transgenic mice and $Gαq^{+/–}$ mice with heterozygous CASR-deficient ($CASR^{+/–}$) mice. Although the basal PTH, calcium and phosphorus values in wild-type animals differed between the various groups, likely reflecting differences in genetic background and age of the mice; the percentage increments in PTH were similar in $Tg^{PTHp–Gqloop}$ transgenic, $Gαq^{+/–}$, and $CASR^{+/–}$ mice (Table 1).

Loss of one CASR allele also resulted in an approximate twofold increase in serum PTH levels, with no significant changes in concentration of serum calcium, phosphate (Table 1), or urinary calcium (data not shown).

Dynamic assessment of parathyroid gland function in $Tg^{PTHp–Gqloop}$ transgenic mice: response to hypo- and hypercalcemia

To define the role of Gαq in regulating PTH secretion in the parathyroid gland, we respectively raised or lowered serum calcium by calcium infusions or EDTA administration. The administration of EGTA resulted in similar reductions in serum calcium in both wild-type and $Tg^{PTHp–Gqloop}$ mice (Figure 3a). In contrast, hypocalcemia stimulated serum PTH (Figure 3b), but the percentage increment of PTH level was less in $Tg^{PTHp–Gqloop}$ transgenic mice (246% compared to 387% wild type), due to their higher baseline PTH values (Figure 3b).

Administration of calcium gluconate to elevate serum calcium (Figure 3a) resulted in similar reductions in serum PTH between transgenic and wild-type mice (that is, reductions of 82.1% in $Tg^{PTHp–Gqloop}$ transgenic mice and 77.6% in wild-type littermates; Figure 3b). We also constructed calcium-PTH curves to assess the sensitivity of the parathyroid glands to changes in extracellular calcium. This analysis demonstrated compared to wild-type mice (Figure 4a) that $Tg^{PTHp–Gqloop}$ mice had lower serum PTH levels as a function of serum calcium (that is, reduction in slope; Figure 4b), indicating that the overexpression of the Gαqloop resulted in parathyroid glands that were less sensitive to changes in serum calcium.

The role of the Gαq subunit in regulating parathyroid gland size

To examine the effect of Gαq on parathyroid gland hyperplasia, we assessed total parathyroid gland size by microscopic *in situ* visualization of mice selectively expressing enhanced green fluorescent protein (eGFP) in the parathyroid glands. These mice were created by crossing PTH-Cre transgenic mice onto ROSA26-rtTA-IRES-EGFP mice. These mice were intercrossed with $Tg^{PTHp–Gqloop}$ mice to create $Tg^{PTHp–Cre}$/ROSA26-rtTA-IRES-EGFP/WT and $Tg^{PTHp–Cre}$/ROSA26-rtTA-IRES-EGFP/$Tg^{PTHp–Gqloop}$ mice. Overexpression of Gαqloop under the control of the PTH promoter resulted in larger parathyroid glands (Figure 5a). The increase in parathyroid gland size was confirmed in serial histological sections of thyroid/parathyroid tissue (Figure 5b). In addition, $Tg^{PTHp–Gqloop}$ mice displayed an increase in the number of parathyroid chief cells. The level of PTH mRNA expression was also increased in $Tg^{PTHp–Gqloop}$ transgenic mice by both reverse transcription (RT)–PCR (Figure 6a) and real-time RT-PCR (Figure 6c). CASR mRNA levels were also increased in the parathyroid gland from $Tg^{PTHp–Gqloop}$ transgenic mice. In contrast, there was a decrease in the expression of CASR in the kidney of $Tg^{PTHp–Gqloop}$ mice compared to wild-type littermates (Figure 6b and c), suggesting that primary alterations in PTG-mediated PTH secretion can result in adaptive changes in the expression of CASR by the kidney.

DISCUSSION

We successfully created a $Tg^{PTHp–Gqloop}$ mouse in which the PTH promoter drives the selective expression of a dominant-negative Gαqloop minigene to the parathyroid gland. Our strategy exploits the previously reported effects of a C-terminal peptide of Gαq, which contains the region of the Gα subunit that interacts with the intracellular domains of agonist-occupied receptors and disrupt this signaling pathway,[25] to achieve parathyroid gland-specific inhibition of Gαq-mediated signaling. Selective disruption of Gαq function in the parathyroid gland resulted in the development of moderately hyperparathyroidism, characterized by increased circulating PTH levels and parathyroid gland enlargement (Figures 2-5). Moreover, the effects on serum PTH levels in $Tg^{PTHp–Gqloop}$ mice were similar to heterozygous Gαq-deficient and CASR-deficient mice (Table 1).

CASR, through either Gαq or Gαi, regulates parathyroid cell hyperplasia, hypertrophys and PTH secretion. Our findings suggest that the Gαq pathway is responsible for parathyroid cell growth, as disruption of this pathway resulted in significant parathyroid gland enlargement caused by hyperplasia. We did not measure PTH content of the PTG, so we do not have precise information regarding hypertrophy. With regard to PTH secretion, the overexpression of the dominant-negative Gαq construct resulted in an alteration in the slope of the calcium-PTH relationship, consistent with reduced sensitivity of the parathyroid gland to secrete PTH in response to changes in extracellular calcium (Figure 4). The inhibition of Gαq, however, did not prevent the maximum secretion of PTH in response to hypocalcemia, indicating that the disruption of CASR-dependent function was incomplete or that the enlargement of the PTG was able to compensate for the reduced CASR function.

In contrast to our findings, the complete ablation of Gαq and Gα11 resulted in severe hyperparathyroidism,[28] similar to that observed in homozygous $CASR^{-/-}$ mice.[29] The failure to observe a more severe degree of hyperparathyroidism in $Tg^{PTHp–Gqloop}$ mice, therefore, likely reflects either residual Gαq activity, the effects of the Gαi, or other signaling pathways that are not targeted by the dominant-negative Gαqloop construct. It is also important to note that unlike the specificity of deleting CASR, the overexpression of the dominant-negative Gαq(305−359) construct would globally disrupt Gαq-dependent signaling from any G-protein-coupled receptors in the parathyroid, including purinergic receptors that are expressed in the parathyroid gland (GEO database: GDS1086) and have been shown to mobilize calcium in parathyroid cells.[30] In any event, there was an increase in chief cell number and amount of PTH mRNA per gland of selective $Tg^{PTHp–Gqloop}$ mice, indicating that even less than maximal reductions in Gαq signaling is sufficient to stimulate parathyroid gland hyperplasia, and PTH gene transcription.

Interestingly, unlike $CASR^{+/-}$ mice that had significant increases in serum calcium compared to wild-type littermates, $Tg^{PTHp–Gqloop}$ mice displayed a slight but not significant increase in serum calcium (Table 1). The reason for the lack of relative hypercalcemia in the $Tg^{PTHp–Gqloop}$ mice may reflect differences in CASR function in the kidney, which is disrupted in the $CASR^{+/-}$ mice but intact in the $Tg^{PTHp–Gqloop}$ mice. The downregulation of CASR message levels in the kidney of $Tg^{PTHp–Gqloop}$ mice is also consistent with ligand-dependent downregulation of CASR. However, we failed to observed differences in the urinary calcium/Cr ratio of $CASR^{+/-}$ mice and $Tg^{PTHp–Gqloop}$ compared to their respective wild-type control mice. The mechanism underlying the decrease in CASR expression in the kidney is not known. However, as PTH acting on PTH receptors in the distal convoluted tubule and connecting tubule stimulates active renal Ca^{2+} reabsorption by the kidney;[31] and CASR acting in the thick ascending limb of the loop of Henle inhibits calcium reabsorption,[32] the observed reduction of CASR would work in concert with elevated PTH to limit renal calcium excretion. In addition, we failed to observe any effects of elevated PTH on bone mineral density. We did not perform a more detailed histomorphometic analysis to detect the effects of elevated PTH on bone.

We also observed an increase in CASR message expression in the parathyroid glands of $Tg^{PTHp–Gqloop}$ mice (Figure 5). From our studies, we cannot determine if this represents an upregulation of CASR expression by disruption of the Gαq signaling or simply reflects the increase in parathyroid growth. The increase in CASR expression in our studies, however, are opposite to the relative reduction of CASR expression in parathyroids of double Gαq/Gα11 knockout mice.[28] In addition, it is possible that the increase in CASR expression may have mitigated the increase in PTH, thereby contributing to the milder degree of hyperparathyroidism in $Tg^{PTHp–Gqloop}$ mice.

The current studies do not define the role of Gαi in mediating the effects of CASR on parathyroid cell function. However, the greater effect of Gαq on gland size and PTH mRNA expression is consistent with its role in cell proliferation and hypertrophy, whereas the relative preservation of maximal PTH secretion in $Tg^{PTHp–Gqloop}$ mice implicates a possible role of Gαi in the PTH secretion. Further studies that target Gαi are needed to explore the likelihood that different Gα subunits have both distinct and overlapping roles in the parathyroid gland.

In conclusion, we have successfully developed a mouse model of hyperparathyroidism caused by parathyroid-specific inhibition of the Gαq. In addition, we show that Gαq has important effects to regulate parathyroid cell growth and PTH mRNA levels, as well as PTH secretion. Using a similar approach to target Gαi and other pathways in parathyroid gland will lead to new insights into specific molecular mechanisms controlling parathyroid gland function in a biologically relevant context.

MATERIALS AND METHODS

Cell culture

HEK-293 cells were grown in Dulbecco's modified Eagle's medium supplemented with 10% fetal calf serum and 1% penicillin/streptomycin at 37 °C in a humidified atmosphere of 95% air and 5% CO_2.

Sources and construction of expression plasmids

The rat CASR cDNA was obtained from Dr AM Snowman and Dr SH Snyder[33] and subcloned in the mammalian expression vector pcDNA3 (Invitrogen, Carlsbad, CA, USA) as previously described.[34] The Gαq(305−359) minigene construct that correspond to the C-terminal peptide sequence of Gαq residues 305−359 was kindly provided by Dr Robert J Lefkowitz from Duke University.[25] We used the previously described SRE-luciferase plasmid DNA as reporter gene.[35]

Transient and stable transfection

For these studies, all plasmid DNAs as described above, were prepared using the EndoFree plasmid maxi kit (Qiagen Inc., Valencia, CA, USA). Transient transfections were preformed as follows: 2×10^5 HEK-293 were plated in the six-well plate and incubated overnight at 37 °C. A DNA-liposome complex was prepared by mixing DNA of the SRE-luciferase reporter plasmid, pCMV-*β*-gal and other expression vector as indicated with TransFast transfection reagent (1:2 DNA/TransFast transfection reagent; Promega Corp., Madison, WI, USA) in Opti-MEM I reduced serum medium (Life Technologies, Inc., Carlsbad, CA, USA). The total plasmid DNA was equalized in each well of six-well plate by adjusting the total amount of DNA to 2 μg per well with the empty vector.

Assessment of agonist-stimulated SRE activity

Quiescence of transfected cells was achieved in subconfluent cultures by incubation for 24 h in serum-free Dulbecco's modified Eagle's medium/F12 containing 0.1% bovine serum albumin. After 2 days of transfection, quiescent cells were treated with vehicle or stimulated for the last 8 h with appropriate agonists as indicated. Luciferase activity was assessed after 8 h of stimulation and measured using the luciferase assay system (Promega Corp., Madison, WI, USA), following the manufacturer's protocol using a BG-luminometer (Gem Biomedical Inc., Hamden, CT, USA).

Gαq knockout mice

Mice were maintained and used in accordance with recommendations in the Guide for the Care and Use of Laboratory Animals, prepared by the Institute on Laboratory Animal Resources, National Research Council (DHHS Publication NIH 86−23, 1985), and by guidelines established by the institutional animal care and use committee of University of Kansas Medical Center.

Gαq knockout mice were obtained from Dr Offermanns of Freie Universität Berlin, Germany.[27] $Tg^{PTH–Cre}$ (ref. [36]) and ROSA26-rtTA-IRES-EGFP mice[37] were purchased from The Jackson Laboratory (Bar Harbor, ME, USA).

Generation of transgenic mice

The transgene was constructed in the pW1 vector, which contains a multiple cloning site and an SV40 intron plus polyadenylation site flanked by the rare restriction enzyme sites *Not*I and *Sfi*I.[38] A 5221-bp fragment of the *hPTH* promoter[39] was released from pBS-5′PTH by restriction endonuclease digestion and subcloned into the blunted *Sac*I site and *Sma*I site of

pW1, thereby generating pW1−5′hPTHp. The pW1−5′hPTHp-Gaqloop construct was constructed by inserting a 165-bp fragment of the C-terminal peptide sequence of mouse Gαq, residues 305−359,[25] was generated by RT–PCR and subcloned into *Xho*I site and *Bam*HI site of pW1−5′hPTHp. Plasmid DNA was first isolated using the Qiafilter Maxi Kit (Qiagen, Valencia, CA, USA), followed by CsCl banding. 5′hPTHp-Gαqloop DNA for microinjection was released from the vector backbone using *Not*I and *Sfi*I, separated by agarose gel, and then gel-purified using Qiaex II gel extraction (Qiagen) according to the manufacturer's instructions. 5′hPTHp-Gαqloop DNA was further purified using the EndoFree Kit (Qiagen) to remove endotoxins and quantified using the PicoGreen Assay Kit (Molecular Probes, Carlsbad, CA, USA). Transgenic mice were made by the Duke Transgenic Facility by microinjecting C57Bl6F1/J fertilized mouse eggs with DNA at a concentration of 2−3 ng/μl according to standard techniques.[40] For genotyping of the $Tg^{PTHp–Gqloop}$ transgenic mice, we used a primer set that forward primer (mouseGαqloop.For: acgcgtcgaccatggctcgagaattcatcc) is located in the 3′ end of Gαq minigene and reverse primer (SV40pA.Rev2: atcagttccataggttggaatc) is located in the downstream poly A sequence region to genotype the $Tg^{PTHp–Gqloop}$ transgenic mice by PCR.

To create triple transgenic mice, we used the following mouse breeding strategies. First, we mated $Tg^{PTH–Cre}$ and $Tg^{PTHp–Gqloop}$ transgenic mice to create the double $Tg^{PTH–Cre}$/$Tg^{PTHp–Gqloop}$ transgenic mice, then mated the ROSA26-rtTA-IRES-EGFP male homozygous mice with double heterozygous $Tg^{PTH–Cre}$/$Tg^{PTHp–Gqloop}$ transgenic female mice to generate triple transgenic $Tg^{PTHp–Cre}$/ROSA26-rtTA-IRES-EGFP/$Tg^{PTHp–Gqloop}$, and their littermates double transgenic $Tg^{PTHp–Cre}$/ROSA26-rtTA-IRES-EGFP/WT mice. Mice were genotyped by PCR using the following primer sets. For $Tg^{PTHp–Gqloop}$ transgene, the forward primer: mouseGaqloop. For acgcgtcgaccatggctcgagaattcatcc and reverse primer: SV40pA.Rev2: atcagttccataggttggaatc. For $Tg^{PTHp–Cre}$ transgene, the PTH-Cre wt1: ctaggccacagaattgaaagatct and PTH-Cre wt2: gtaggtggaaattctagcatcatcc as internal control for wild-type mice. The PTH-Cre tgp1: gcggtctggcagtaaaaactatc and PTH-Cre tgp2: gtgaaacagcattgctgtcactt for the Cre transgene. For ROSA26-rtTA-IRES-EGFP mice, the oIMR0872: aagttcatctgcaccaccg and oIMR1416: tccttgaagaagatggtgcg amplifying eGFP transgene, the oIMR3621: cgtgatctgcaactccagtc and oIMR3622: ggagcgggagaaatggatatg amplifying wild-type allele.

PIXImus bone mineral density analysis

Bone mineral density of whole skeletons and femurs were assessed at 8 weeks of age using a PIXImus bone densitometer (Lunar Corp., Madison, WI, USA) as previously described.[41]

Serum and urine biochemistries

Serum and urinary calcium and phosphate as well as serum PTH were measured, respectively, using Calcium Liquicolor (Stanbio Laboratory, Boerne, TX, USA), the phosphomolybdate-ascorbic acid method, and the Mouse Intact PTH ELISA Kit (Immunotopics, San Clemente, CA, USA) as described previously.[41] Creatinine was measured by the colorimetric alkaline picrate method (Sigma kit 555, Sigma, St. Louis, MO, USA).

Quantitative real-time RT-PCR and RT–PCR

For quantitative real-time RT-PCR, 2.0 μg total RNA isolated from kidney and thyroid include parathyroid of 8-week-old wild-type and $Tg^{PTHp–Gqloop}$ transgenic mice was reverse transcribed as described.[42] PCR reactions contained 100 ng template, 300 n_M each forward and reverse primer and 1X iQ SYBR Green Supermix (Bio-Rad, Hercules, CA, USA) in 50 μl. Samples were amplified for 40 cycles in an iCycler iQ Real-Time PCR Detection System with an initial melt at 95 °C for 10 min followed by 40 cycles of 95 °C for 15 s and 60 °C for 1 min. PCR product accumulation was monitored at multiple points during each cycle by measuring the increase in fluorescence caused by the binding of SybrGreen I to dsDNA. The threshold

cycle (C_t) of tested-gene product from the indicated genotype was normalized to the C_t for cyclophilin A.

Reverse transcription–PCR was done using two-step RNA PCR (PerkinElmer, Waltham, MA, USA). In separate reactions, 2.0 μg of DNase-treated total RNA was reverse-transcribed into cDNA with the respective reverse primers specified below and Moloney murine leukemia virus reverse transcriptase (Life Technologies Inc., Carlsbad, CA, USA). The products of first-strand cDNA synthesis were directly amplified by PCR using AmpliTaq DNA polymerase (PerkinElmer). The following primer sets were used to amplify targeting genes. For mouse *PTH* gene, PTH.26.For: agtccaattcatcag ttgtc and PTH.235.Rev: atgcataagctgtatttcac. For mouse *CASR* gene, mCASR.For: tcgagacccctacatggac and mCASR.Rev: aaattcaggtgccgtaggtg. For housekeeping gene control *G3PDH* gene, G3PDH.F143: gacccctcattgacctcaactaca and G3PDH.R1050: ggtcttactccttggaggccatgt.

Western blot

Mouse parathyroid gland lysates were denatured in Laemmli sample buffer, then resolved on NuPAGE Novex 12% Bis-Tris gels and transferred to nitrocellulose membrane (Invitrogen). Filters were probed with rabbit polyclonal antisera raised to the Gαq C terminus (amino acids 341−359; Santa Cruz Biotechnology, Santa Cruz, CA, USA), and anti-rabbit secondary antibody (Cell Signaling Technology, Boston, MA, USA). The immunostained bands will be visualized using an ECL plus Western Blotting Detection System following manufacturer's instructions (Amersham, Piscataway, NJ, USA).

Parathyroid gland histological analysis

For histological analysis, we have found it to be most reliable to obtain an in-block section of the mouse neck to include the thyroid, parathyroid glands, trachea, and surrounding muscle and soft tissue. The resected tracheal blocks from wild-type and $Tg^{PTHp–Gqloop}$ transgenic mice were dissected, dehydrated, embedded in paraffin, sectioned (8 μm), and stained hematoxylin/eosin.

PTH–calcium relationship analysis by intraperitoneal injection method

After fasting for 5−6 h, each mouse was administered a single intraperitoneal injection of ether 300 μmol/kg body weight of EGTA or calcium gluconate. The blood samples were collected 30 min after the administration of EGTA and 1 h after the administration of calcium gluconate for measurement of serum PTH and total calcium levels.[43]

Statistical analysis

We evaluated differences between groups by one-way analysis of variance. All values are expressed as means±s.e.m. All computations were performed using the Statgraphic statistical graphics system (STSC Inc., Rockville, MD, USA).

ACKNOWLEDGMENTS

This work was supported by NIH R01-AR37308 (L Darryl Quarles) and COBRE grant P20 RR017686 (Min Pi).

REFERENCES

1. Brown EM, Gamba G, Riccardi D, et al. Cloning and characterization of an extracellular Ca(2+)-sensing receptor from bovine parathyroid. Nature 1993;366:575–580. [PubMed: 8255296]
2. Brauner-Osborne H, Jensen AA, Sheppard PO, et al. Cloning and characterization of a human orphan family C G-protein coupled receptor GPRC5D. Biochim Biophys Acta 2001;1518:237–248. [PubMed: 11311935]

3. Pollak MR, Brown EM, Chou YH, et al. Mutations in the human Ca(2+)-sensing receptor gene cause familial hypocalciuric hypercalcemia and neonatal severe hyperparathyroidism. Cell 1993;75:1297–1303. [PubMed: 7916660]
4. Bai M, Quinn S, Trivedi S, et al. Expression and characterization of inactivating and activating mutations in the human Ca2+o-sensing receptor. J Biol Chem 1996;271:19537–19545. [PubMed: 8702647]
5. Chou YH, Pollak MR, Brandi ML, et al. Mutations in the human Ca(2+)-sensing-receptor gene that cause familial hypocalciuric hypercalcemia. Am J Hum Genet 1995;56:1075–1079. [PubMed: 7726161]
6. Hendy GN, D'Souza-Li L, Yang B, et al. Mutations of the calcium-sensing receptor (CASR) in familial hypocalciuric hypercalcemia, neonatal severe hyperparathyroidism, and autosomal dominant hypocalcemia. Hum Mutat 2000;16:281–296. [PubMed: 11013439]
7. Hauache OM, Hu J, Ray K, et al. Effects of a calcimimetic compound and naturally activating mutations on the human Ca2+ receptor and on Ca2+ receptor/metabotropic glutamate chimeric receptors. Endocrinology 2000;141:4156–4163. [PubMed: 11089548]
8. Quarles LD. Cinacalcet HCl: a novel treatment for secondary hyperparathyroidism in stage 5 chronic kidney disease. Kidney Int Suppl 2005;96:S24–S28. [PubMed: 15954947]
9. Cunningham J, Danese M, Olson K, et al. Effects of the calcimimetic cinacalcet HCl on cardiovascular disease, fracture, and health-related quality of life in secondary hyperparathyroidism. Kidney Int 2005;68:1793–1800. [PubMed: 16164656]
10. Chen CJ, Barnett JV, Congo DA, et al. Divalent cations suppress 3′, 5′-adenosine monophosphate accumulation by stimulating a pertussis toxin-sensitive guanine nucleotide-binding protein in cultured bovine parathyroid cells. Endocrinology 1989;124:233–239. [PubMed: 2462488]
11. Brown E, Enyedi P, LeBoff M, et al. High extracellular Ca2+ and Mg2+ stimulate accumulation of inositol phosphates in bovine parathyroid cells. FEBS Lett 1987;218:113–118. [PubMed: 3109945]
12. Huang C, Hujer KM, Wu Z, et al. The Ca2+-sensing receptor couples to Galpha12/13 to activate phospholipase D in Madin-Darby canine kidney cells. Am J Physiol Cell Physiol 2004;286:C22–C30. [PubMed: 12954603]
13. Brown EM. Extracellular Ca2+ sensing, regulation of parathyroid cell function, and role of Ca2+ and other ions as extracellular (first) messengers. Physiol Rev 1991;71:371–411. [PubMed: 2006218]
14. Kifor O, Diaz R, Butters R, et al. The Ca2+-sensing receptor (CaR) activates phospholipases C, A2, and D in bovine parathyroid and CaR-transfected, human embryonic kidney (HEK293) cells. J Bone Miner Res 1997;12:715–725. [PubMed: 9144337]
15. Handlogten ME, Huang C, Shiraishi N, et al. The Ca2+-sensing receptor activates cytosolic phospholipase A2 via a Gqalpha-dependent ERK-independent pathway. J Biol Chem 2001;276:13941–13948. [PubMed: 11278341]
16. McNeil SE, Hobson SA, Nipper V, et al. Functional calcium-sensing receptors in rat fibroblasts are required for activation of SRC kinase and mitogen-activated protein kinase in response to extracellular calcium. J Biol Chem 1998;273:1114–1120. [PubMed: 9422777]
17. Quarles LD, Hartle JE II, Siddhanti SR, et al. A distinct cation-sensing mechanism in MC3T3-E1 osteoblasts functionally related to the calcium receptor. J Bone Miner Res 1997;12:393–402. [PubMed: 9076582]
18. Huang C, Handlogten ME, Miller RT. Parallel activation of phosphatidylinositol 4-kinase and phospholipase C by the extracellular calcium-sensing receptor. J Biol Chem 2002;277:20293–20300. [PubMed: 11907035]
19. Pi M, Oakley RH, Gesty-Palmer D, et al. Beta-arrestin- and G protein receptor kinase-mediated calcium-sensing receptor desensitization. Mol Endocrinol 2005;19:1078–1087. [PubMed: 15637145]
20. Pi M, Spurney RF, Tu Q, et al. Calcium-sensing receptor activation of rho involves filamin and rho-guanine nucleotide exchange factor. Endocrinology 2002;143:3830–3838. [PubMed: 12239094]
21. Neves SR, Ram PT, Iyengar R. G protein pathways. Science 2002;296:1636–1639. [PubMed: 12040175]

22. Peavy RD, Hubbard KB, Lau A, et al. Differential effects of Gq alpha, G14 alpha, and G15 alpha on vascular smooth muscle cell survival and gene expression profiles. Mol Pharmacol 2005;67:2102–2114. [PubMed: 15788742]
23. Stork PJ, Schmitt JM. Crosstalk between cAMP and MAP kinase signaling in the regulation of cell proliferation. Trends Cell Biol 2002;12:258–266. [PubMed: 12074885]
24. Yamaguchi T, Wallace DP, Magenheimer BS, et al. Calcium restriction allows cAMP activation of the B-Raf/ERK pathway, switching cells to a cAMP-dependent growth-stimulated phenotype. J Biol Chem 2004;279:40419–40430. [PubMed: 15263001]
25. Akhter SA, Luttrell LM, Rockman HA, et al. Targeting the receptor-Gq interface to inhibit *in vivo* pressure overload myocardial hypertrophy. Science 1998;280:574–577. [PubMed: 9554846]
26. West RE Jr, Moss J, Vaughan M, et al. Pertussis toxin-catalyzed ADP-ribosylation of transducin. Cysteine 347 is the ADP-ribose acceptor site. J Biol Chem 1985;260:14428–14430. [PubMed: 3863818]
27. Offermanns S, Zhao LP, Gohla A, et al. Embryonic cardiomyocyte hypoplasia and craniofacial defects in G alpha q/G alpha 11-mutant mice. EMBO J 1998;17:4304–4312. [PubMed: 9687499]
28. Wettschureck N, Lee E, Libutti SK, et al. Parathyroid-specific double knockout of Gq and G11 alpha-subunits leads to a phenotype resembling germline knockout of the extracellular Ca2+ -sensing receptor. Mol Endocrinol 2007;21:274–280. [PubMed: 16988000]
29. Garner SC, Pi M, Tu Q, et al. Rickets in cation-sensing receptor-deficient mice: an unexpected skeletal phenotype. Endocrinology 2001;142:3996–4005. [PubMed: 11517179]
30. Gibb CA, Cook DI, Delbridge L, et al. Pharmacological characterization of the nucleotide receptors that mobilize Ca2+ ions in human parathyroid cells. J Endocrinol 1994;142:277–283. [PubMed: 7931001]
31. van Abel M, Hoenderop JG, van der Kemp AW, et al. Coordinated control of renal Ca(2+) transport proteins by parathyroid hormone. Kidney Int 2005;68:1708–1721. [PubMed: 16164647]
32. Bushinsky DA, Laplante K, Asplin JR. Effect of cinacalcet on urine calcium excretion and supersaturation in genetic hypercalciuric stone-forming rats. Kidney Int 2006;69:1586–1592. [PubMed: 16557225]
33. Ruat M, Molliver ME, Snowman AM, et al. Calcium sensing receptor: molecular cloning in rat and localization to nerve terminals. Proc Natl Acad Sci USA 1995;92:3161–3165. [PubMed: 7724534]
34. Spurney RF, Pi M, Flannery P, et al. Aluminum is a weak agonist for the calcium-sensing receptor. Kidney Int 1999;55:1750–1758. [PubMed: 10231437]
35. Yamauchi K, Holt K, Pessin JE. Phosphatidylinositol 3-kinase functions upstream of Ras and Raf in mediating insulin stimulation of c-fos transcription. J Biol Chem 1993;268:14597–14600. [PubMed: 8392056]
36. Libutti SK, Crabtree JS, Lorang D, et al. Parathyroid gland-specific deletion of the mouse Men1 gene results in parathyroid neoplasia and hypercalcemic hyperparathyroidism. Cancer Res 2003;63:8022–8028. [PubMed: 14633735]
37. Belteki G, Haigh J, Kabacs N, et al. Conditional and inducible transgene expression in mice through the combinatorial use of Cre-mediated recombination and tetracycline induction. Nucleic Acids Res 2005;33:e51. [PubMed: 15784609]
38. Liu S, Guo R, Tu Q, et al. Overexpression of Phex in osteoblasts fails to rescue the Hyp mouse phenotype. J Biol Chem 2002;277:3686–3697. [PubMed: 11713245]
39. Imanishi Y, Hosokawa Y, Yoshimoto K, et al. Primary hyperparathyroidism caused by parathyroid-targeted overexpression of cyclin D1 in transgenic mice. J Clin Invest 2001;107:1093–1102. [PubMed: 11342573]
40. Bonnerot C, Nicolas JF. Application of LacZ gene fusions to postimplantation development. Methods Enzymol 1993;225:451–469. [PubMed: 7901738]
41. Tu Q, Pi M, Karsenty G, et al. Rescue of the skeletal phenotype in CasR-deficient mice by transfer onto the Gcm2 null background. J Clin Invest 2003;111:1029–1037. [PubMed: 12671052]
42. Xiao ZS, Simpson LG, Quarles LD. IRES-dependent translational control of Cbfa1/Runx2 expression. J Cell Biochem 2003;88:493–505. [PubMed: 12532326]
43. Imanishi Y, Hall C, Sablosky M, et al. A new method for *in vivo* analysis of parathyroid hormone-calcium set point in mice. J Bone Miner Res 2002;17:1656–1661. [PubMed: 12211436]

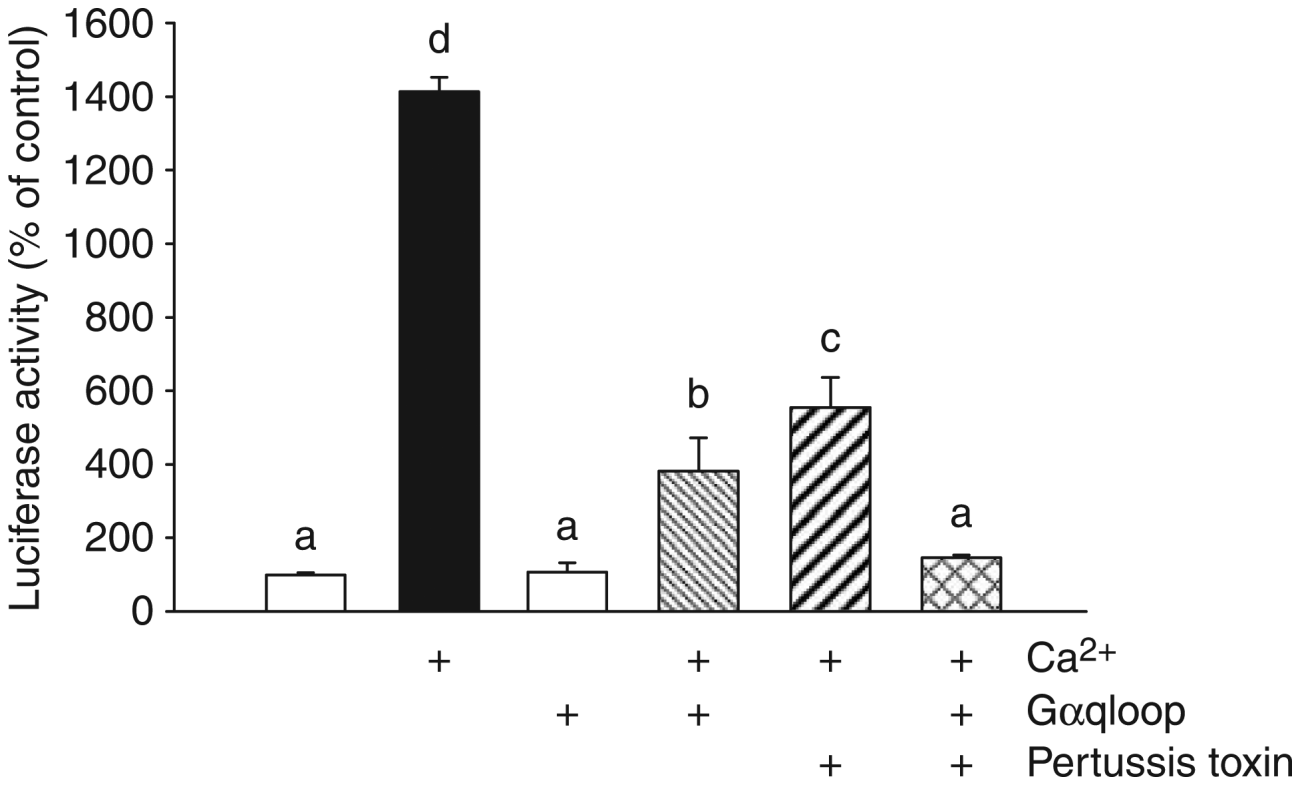

Figure 1. CASR is coupled to activation of Gαq and Gαi

HEK-293 stably CASR-expressing cells were cotransfected with the constructs directing the expression of Gαqloop (corresponding to residues 305−359 of mouse Gαq; 1.5 μg), the SRE-luciferase reporter gene (0.5 μg) and *p*-cytomegalovirus-β-galactosidase (pCMV-β-gal; 0.015 μg) per well of six-well plate. The transfection is described in 'Materials and Methods'. After 2 days of transfection, quiescent cells were pretreated with vehicle or 100 ng/ml pertussis toxin for 5 h, then stimulated by 5 mM calcium for the last 8 h. Data are shown as relative luciferase activity reported as the percent induction, compared with the activity under nonstimulated conditions and normalized for β-galactosidase. Values represent the mean±s.e.m. of at least three experiments. Values sharing the same superscript are not significantly different at $P \leq 0.05$.

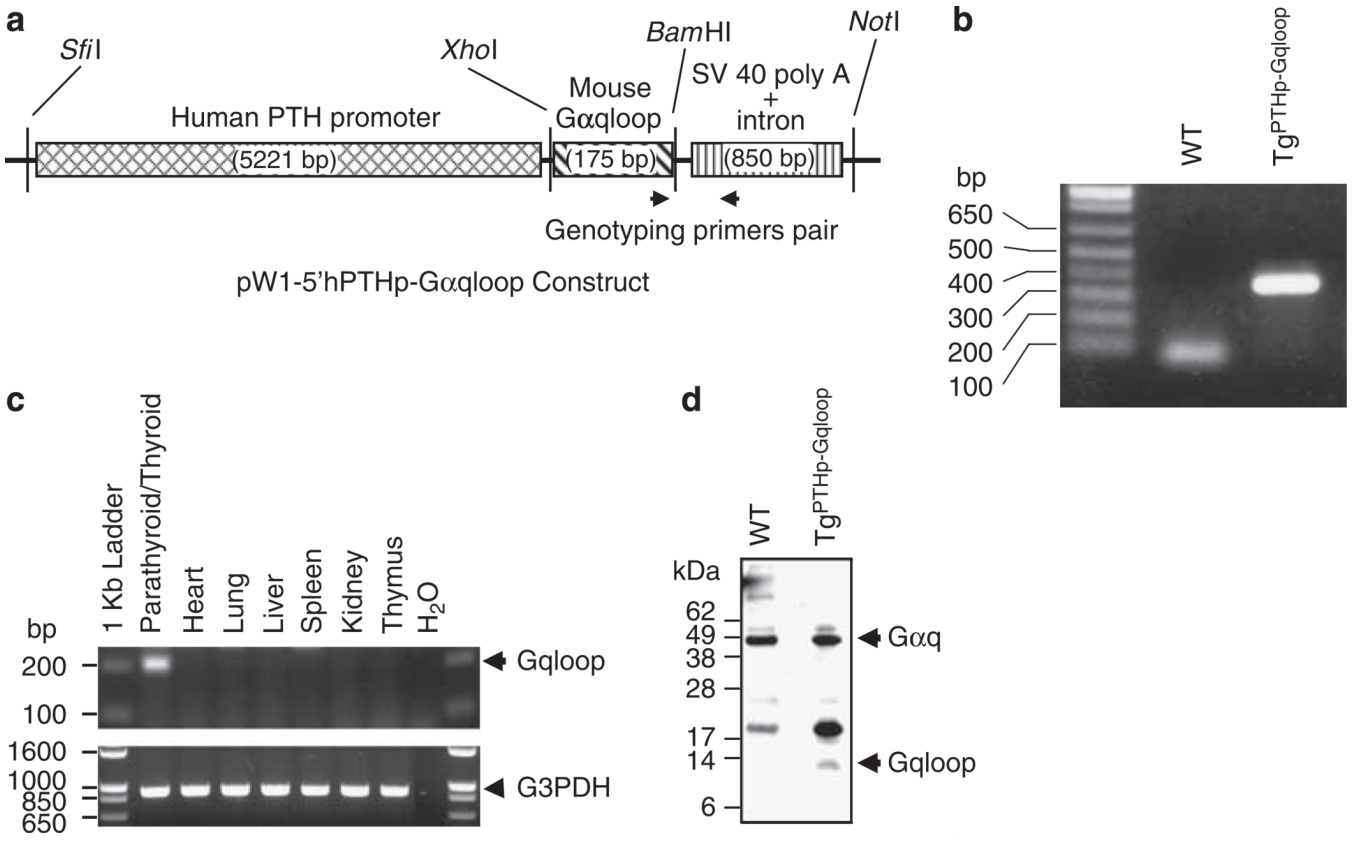

Figure 2. Targeted expression of dominant-negative Gαqloop minigene to mouse parathyroid glands

(**a**) Schematic of transgenic construct consisting of the human PTH promoter driving the expression of the dominant-negative Gαqloop minigene. (**b**) Genotyping of the $Tg^{PTHp–Gqloop}$ transgenic mice by PCR. The forward and reverse primers are respectively located in the 3′ end of Gαq minigene and in the downstream poly A sequence region. Tissue-restricted expression of Gαqloop transgene by RT–PCR (**c**) and Western blot analysis (**d**).

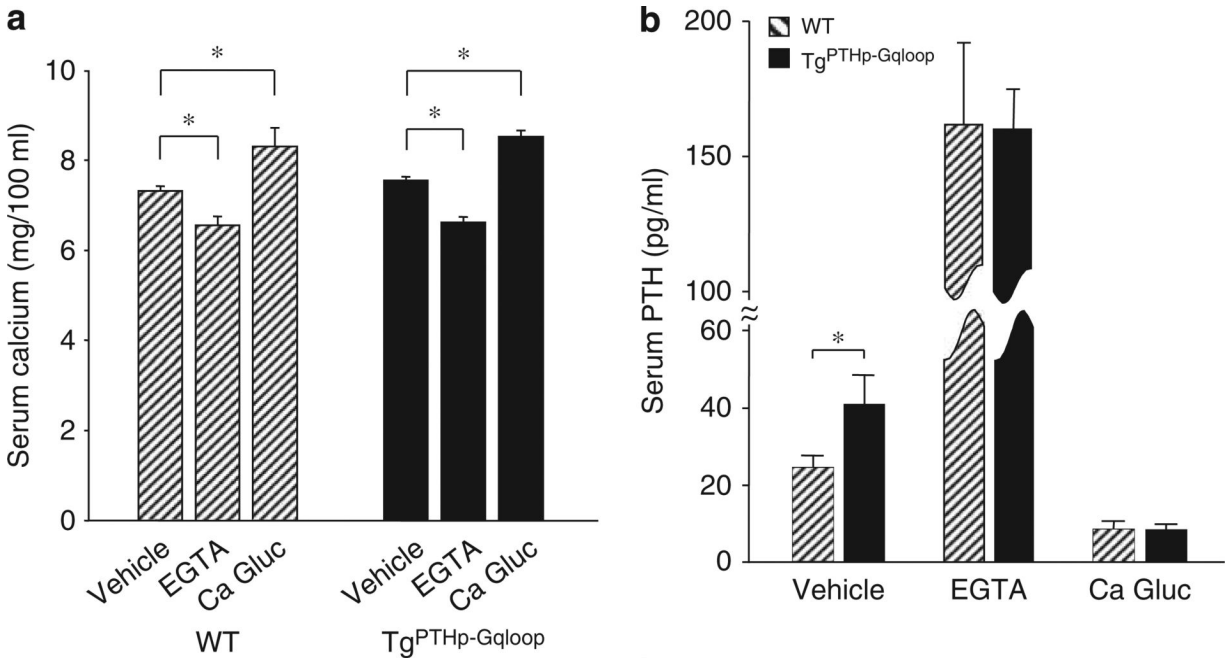

Figure 3. Effects of Gαqloop on PTH secretion

WT and $Tg^{PTHp–Gqloop}$ transgenic mice were subjected to EGTA-induced hypocalcemia or calcium gluconate (Ca Gluc)-induced hypercalcemia as described in 'Materials and Methods'. (**a**) Total serum calcium and (**b**) PTH concentrations in wild-type (WT) and $Tg^{PTHp–Gqloop}$ transgenic mice after EGTA or calcium gluconate intraperitoneal injection. Data are mean ±s.e.m. from 6 to 10 individual mice. *Significant difference between vehicle and EGTA or calcium gluconate treatment group mice at $P<0.05$, respectively. The level of PTH in response to hypocalcemia was similar in wild-type and transgenic mice, but the percentage increment of PTH level was less in $Tg^{PTHp–Gqloop}$ transgenic mice than in wild-type mice (246% and 387%, respectively), due to the higher baseline PTH values in $Tg^{PTHp–Gqloop}$ transgenic mice.

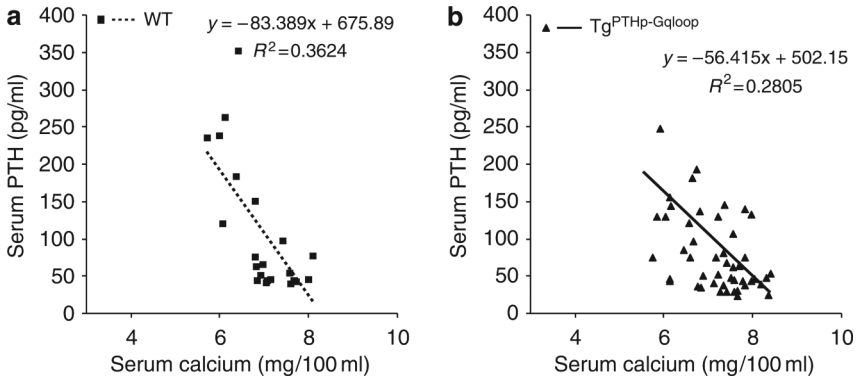

Figure 4. Relationship between serum calcium and PTH levels in wild-type and Tg$^{PTHp–Gqloop}$ transgenic mice

(**a**) Regression analysis showing the normal relationship between serum calcium and PTH levels in wild-type mice. (**b**) Overexpression of the Gαqloop transgene to the parathyroid gland alters the slope of the serum calcium and PTH-level relationship, consistent with impaired calcium sensing.

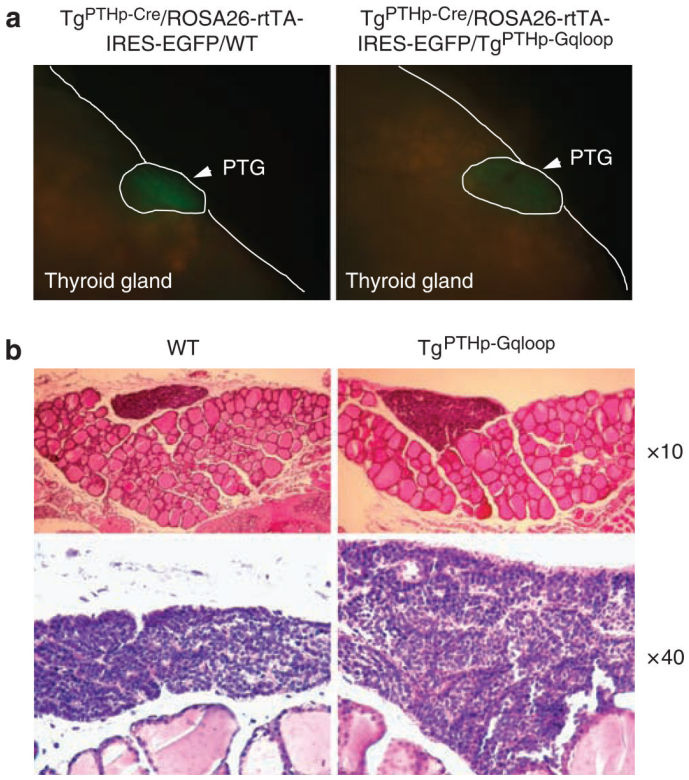

Figure 5. Effects of Gαqloop on proliferation of parathyroid glands

(**a**) Fluorescence microscopy images of the parathyroid gland of control double transgenic $Tg^{PTHp–Cre}$/ROSA26-rtTA-IRES-EGFP/WT and triple transgenic $Tg^{PTHp–Cre}$/ROSA26-rtTA-IRES-EGFP/$Tg^{PTHp–Gqloop}$ mice. Parathryroid glands express eGFP under the control of the ROSA26 promoter (generated by crossing PTH-Cre with ROSA26-rtTA-IRES-EGFP mice). (**b**) Histologic appearance of parathyroid gland from wild-type (WT) mice and $Tg^{PTHp–Gqloop}$ sex-matched littermates. Sections were prepared from adult mice for light microscopy and stained with H&E. The upper panels show original magnification × 10, and the lower panels show magnification × 40 of the thyroid and parathyroid glands from wild-type mice (WT) and $Tg^{PTHp–Gqloop}$ littermates. All mice are 2 months of age. Tissues are formalin fixed and have been stained with H&E.

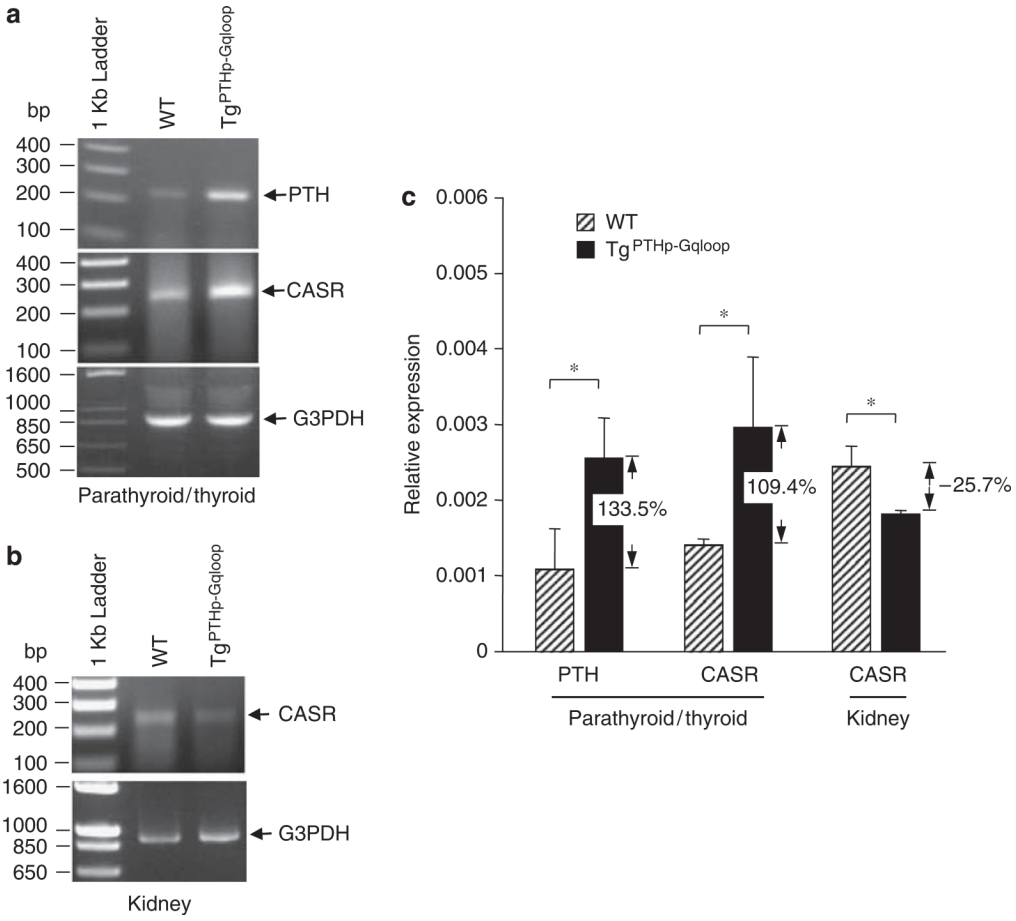

Figure 6. Comparison of *PTH* and *CASR* expression from parathyroid and kidney in wild-type (WT) and $Tg^{PTHp–Gqloop}$ transgenic mice

(**a, b**) RT–PCR and (**c**) Quantitative real-time RT-PCR were performed as described in 'Materials and Methods'. Data are mean±s.e.m. from more than three individual mice. *Significant difference from wild-type and $Tg^{PTHp–Gqloop}$ transgenic mice at $P<0.05$.

Table 1

Comparison of serum PTH, calcium, and phosphorus in wild-type and $Tg^{PTHp–Gqloop}$ transgenic mice, wild-type and $Gαq^{+/–}$ heterozygous mice, and wild-type and $CASR^{+/–}$ heterozygous mice

	Serum		
	PTH (pg/ml)	**Calcium (mg/100 ml)**	**Phosphorus (mg/100 ml)**
WT	25.426 ± 2.478	9.142 ± 0.201	6.433 ± 0.445
$Tg^{PTHp–Gqloop}$	43.419 ± 4.823*	9.458 ± 0.274	5.793 ± 0.281
P-value	0.0212	0.3782	0.2377
WT	10.625 ± 1.806	7.957 ± 0.109	4.292 ± 0.201
$Gαq^{+/–}$	20.574 ± 3.228*	8.076 ± 0.121	4.569 ± 0.174
P-value	0.0128	0.481	0.3007
WT	25.213 ± 2.994	8.097 ± 0.172	8.267 ± 0.379
$CASR^{+/–}$	40.443 ± 4.926*	8.551 ± 0.144	8.244 ± 0.272
P-value	0.0302	0.0547	0.9607

CASR, calcium sensing receptor; PTH, parathyroid hormone; WT, wild type.

Values represent mean ± s.e.m. from more than six individual mice per group.

*Significant difference between WT and $Gαq^{+/–}$ or $Tg^{PTHp–Gqloop}$ or $CASR^{+/–}$ group mice at $P < 0.05$. The serum of WT and $Gαq^{+/–}$ or $Tg^{PTHp–Gqloop}$ was obtained from 8-week-old mice, and the serum of WT and $CASR^{+/–}$ was obtained from 6-week-old mice.